# Determination of the importance of the stereochemistry of psorospermin in topoisomerase II–induced alkylation of DNA and *in vitro* and *in vivo* biological activity

**Ingrid M. Fellows,[1] Michael Schwaebe,[2] Thomas S. Dexheimer,[3] Hariprasad Vankayalapati,[3] Mary Gleason-Guzman,[3] Jeffrey P. Whitten,[2] and Laurence H. Hurley[3,4,5]**

[1]The University of Texas at Austin, Austin, Texas; [2]Cylene Pharmaceuticals, Inc., San Diego, California; and [3]College of Pharmacy and [4]Department of Chemistry, The University of Arizona and [5]The Arizona Cancer Center, Tucson, Arizona

## Abstract

**Psorospermin is a natural product that has been shown to have activity against drug-resistant leukemia lines and AIDS-related lymphoma. It has also been shown to alkylate DNA through an epoxide-mediated electrophilic attack, and this alkylation is greatly enhanced at specific sites by topoisomerase II. In this article, we describe the synthesis of the two diastereomers of $O^5$-methyl psorospermin and their *in vitro* activity against a range of solid and hematopoietic tumors. The diastereomeric pair (±)-(2′*R*,3′*R*) having the naturally occurring enantiomer (2′*R*,3′*R*) is the most active across all the cell lines and shows approximately equal activity in both drug-sensitive and drug-resistant cell lines. In subsequent studies using all four enantiomers of $O^5$-methyl psorospermin, the order of biological potency is (2′*R*,3′*R*) > (2′*R*,3′*S*) = (2′*S*,3′*R*) > (2′*S*,3′*S*). This order of potency is also found in the topoisomerase II–induced alkylation of $O^5$-methyl psorospermin and can be rationalized by molecular modeling of the psorospermin-duplex binding complex. Therefore, this study defines the optimum stereochemical requirements for both the topoisomerase II–induced alkylation of DNA and the biological activity by psorospermin and its $O^5$-methyl derivatives. Finally, (2′*R*,3′*R*) psorospermin was found to be as effective as gemcitabine in slowing tumor growth *in vivo* in a MiaPaCa pancreatic cancer model. In addition, (2′*R*,3′*R*) psorospermin in combination with gemcitabine was found to show an at least additive effect in slowing tumor growth of MiaPaCa. [Mol Cancer Ther 2005;4(11):1729–39]**

## Introduction

Psorospermin (Fig. 1) is a natural product isolated from the roots and stembark of the African plant *Psorospermum febrifugum* (1, 2). The first chiral synthesis of the natural product has been reported recently (3). Psorospermin has been shown to intercalate into the DNA helix and covalently modify guanine at the N7 position in the major groove through an epoxide-mediated electrophilic attack (4). It is active against drug-resistant human leukemia lines and AIDS-related lymphoma.[6] We have shown that psorospermin alkylation at specific sites on DNA is greatly enhanced in the presence of topoisomerase II (5), indicating that the abasic sites on DNA and antitumor activity of psorospermin might be related to its specific interaction with the topoisomerase II-DNA complex. It has also been proposed that psorospermin induces DNA strand breaks, abasic sites, and protein-DNA cross-links (6).

Type II topoisomerases are essential nuclear enzymes that regulate the topological status of DNA (7). The topoisomerase II catalytic cycle consists of several discrete steps. First, topoisomerase II forms a noncovalent complex with duplex DNA. In the presence of $Mg^{2+}$, a dsDNA cleavage and religation equilibrium is then established at the pre-strand passage stage, with a topoisomerase II tyrosine residue attached to the 5′ phosphate of the broken DNA. Next, on the binding of ATP, an intact DNA duplex is passed through the transient double-stranded break site (or ''gate site''). A post-strand passage equilibrium involving DNA breakage and religation is then established. Finally, following the religation, ATP is hydrolyzed to facilitate enzyme turnover and the initiation of a subsequent cycle (8, 9).

We have shown that the enhanced DNA alkylation by psorospermin in the presence of topoisomerase II is dependent on pH but is independent of $Mg^{2+}$ or ATP (10). This suggests that topoisomerase II–mediated psorospermin alkylation occurs in the initial noncovalent binding step in the topoisomerase II catalytic cycle. We also showed that N7 of guanine is still the alkylation site for psorospermin in the presence of topoisomerase II (10). Furthermore, the topoisomerase II-DNA complex trapped by psorospermin is slowly reversible on the addition of excess salt (10).

Received 6/7/05; revised 8/25/05; accepted 9/13/05.

**Grant support:** NIH grant CA49751.

The costs of publication of this article were defrayed in part by the payment of page charges. This article must therefore be hereby marked advertisement in accordance with 18 U.S.C. Section 1734 solely to indicate this fact.

**Requests for reprints:** Laurence H. Hurley, The Arizona Cancer Center, 1515 North Campbell Avenue, Tucson, AZ 85724.
Phone: 520-626-5622; Fax: 520-626-5623.
E-mail: hurley@pharmacy.arizona.edu



doi:10.1158/1535-7163.MCT-05-0183

[6] John Cassady (Ohio State University), personal communication.

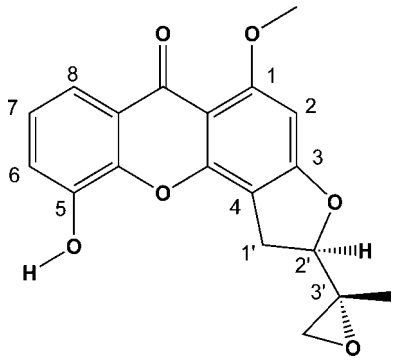

**Figure 1.** Structure of psorospermin.

Because of the apparent novel mechanism of action of psorospermin and its unique profile in the NCI-60 panel screen, we have completed the synthesis of the two diastereomeric pairs of $O^5$-methyl psorospermin as well as the four enantiomeric psorospermin molecules and compared their *in vitro* activity. For the diastereomeric pair of (±)-(2′*R*,3′*R*) $O^5$-methyl psorospermin, which contains an isomer having the same stereochemistry as the natural product, we have examined the *in vitro* activity in a wide range of solid and hematopoietic cell lines. Results show that (±)-(2′*R*,3′*R*) $O^5$-methyl psorospermin is active in both drug-resistant and drug-sensitive cell lines and has a wide spectrum of activity in both hematopoietic and solid tumors. Through chiral separation of the diastereomeric pairs of psorospermin, we have obtained the four chiral compounds, which have been compared for topoisomerase II–enhanced cleavage and *in vitro* activity. Molecular modeling has been used to rationalize the relative topoisomerase II–induced cleavage of DNA and *in vitro* potency of the four enantiomers based on the binding energies and distance between N7 of guanine and the reactive epoxide. Finally, psorospermin was shown to have *in vivo* activity against a MiaPaCa pancreatic cancer model.

## Materials and Methods

### General Procedures

Unless otherwise noted, all starting materials were obtained from commercial suppliers and used without further purification. $Pd(CH_3CN)_4(BF_4)_2$ was obtained from Strem Chemicals (Newburyport, MA). Dimethylformamide and DMSO were purchased 99.8% anhydrous from Aldrich. Benzene was distilled from $CaH_2$. All reactions were run under an argon atmosphere unless noted. The $^1H$ and $^{13}C$ nuclear magnetic resonance (NMR) spectra were determined, unless otherwise indicated, as solutions in $CDCl_3$ at the indicated field; chemical shifts are expressed in parts/million (δ units), referenced to the solvent. Splitting patterns are designated as s (singlet), d (doublet), t (triplet), app t (apparent triplet), q (quartet), sex (sextet), m (multiplet), comp (complex multiplet), and br (broad).

**1,3-Dihydroxy-5-Methoxy Xanthone (1).** Prepared according to the literature procedure (11). All analytic data are satisfactory.

**3-Benzyloxy-1-Hydroxy-5-Methoxy Xanthone.** $Cs_2CO_3$ (10.1 g, 31 mmol) was added in portions to phenol **1** (4.0 g, 15 mmol) and BnBr (1.7 mL, 14 mmol) in dimethylformamide (80 mL) at 0°C. The reaction was warmed to room temperature. After 5 hours, more BnBr was added (0.1 mL) and the reaction was stirred for 36 hours (TLC: 40% ethyl acetate/hexane). The reaction was decanted and washed with $CH_2Cl_2$ into an Erlenmeyer flask that had been placed in an ice-cooled bath. With stirring, 2 mol/L HCl was added slowly until acidic by pH paper. After warming to room temperature, the reaction was diluted with $CH_2Cl_2$ (500 mL) and $H_2O$ (200 mL). The layers were separated and the aqueous layer was reextracted with $CH_2Cl_2$ (2 × 300 mL). The organic layers were combined, washed with brine (200 mL), dried ($Na_2SO_4$), and concentrated under reduced pressure to provide 3.9 g (72%) of a pink solid. $^1H$ NMR (250 MHz, $CDCl_3$) δ 12.8 (s, 1 H), 7.82 (d, 1 H, *J* = 5.9 Hz), 7.42–7.20 (complex, 8 H), 6.64 (s, 1 H), 5.30 (s, 2 H), 4.03 (s, 3 H); $^{13}C$ NMR (62.5 MHz) δ 180.1, 165.6, 163.1, 158.0, 147.0, 145.5, 135.6, 128.6, 128.2, 127.4, 123.4, 121.0, 116.5, 115.4, 104.2, 98.1, 93.3, 70.3, 56.2; mass spectrum (CI) *m/z* + 1 349.1068 [$C_{21}H_{17}O_5$ (M + 1) requires 349.1076] 349 (base), 259.

**3-Benzyloxy-1,5-Dimethoxy Xanthone (2).** $Cs_2CO_3$ (27.0 g, 83 mmol) was added in portions to the phenol (14.5 g, 42 mmol) and methyl iodide (8.0 mL, 125 mmol) in dimethylformamide (400 mL) at room temperature. After 3 hours at 50°C, the reaction was decanted and washed with $CH_2Cl_2$ into an Erlenmeyer that had been placed in an ice-cooled bath. With stirring, 2 mol/L HCl was added slowly until acidic by pH paper. After warming to room temperature, the reaction was diluted with $CH_2Cl_2$ (800 mL) and $H_2O$ (400 mL). The layers were separated and the aqueous layer was reextracted with $CH_2Cl_2$ (300 mL). The organic layers were combined, washed with brine (400 mL), dried ($Na_2SO_4$), and concentrated under reduced pressure to provide a red sludge that was triturated with ethanol and filtered to afford 9.3 g (66%) of **2** as a pink solid. $^1H$ NMR (250 MHz, $CDCl_3$) δ 7.84 (d, 1 H, *J* = 6.0 Hz), 7.42–7.31 (complex, 5 H), 7.20–7.07 (complex, 2 H), 6.63 (s, 1 H), 6.37 (s, 1 H), 5.08 (s, 2 H), 3.92 (s, 3 H), 3.88 (s, 3 H); $^{13}C$ NMR (62.5 MHz) δ 175.2, 163.8, 161.7, 159.4, 147.8, 144.5, 135.6, 128.6, 128.3, 127.5, 123.9, 123.1, 117.5, 114.3, 106.1, 95.9, 93.6, 70.4, 56.3, 56.2; mass spectrum (CI) *m/z* + 1 363.1242 [$C_{22}H_{19}O_5$ (M + 1) requires 363.1232] 363 (base), 339.

**1,5-Dimethoxy-3-(3′3′-Dimethylpropynoxy) Xanthone.** $FeCl_3$ (9.0 g, 69 mmol) was added in portions to **2** (5.0 g, 17 mmol) in $CH_2Cl_2$ (150 mL). After stirring for 40 minutes, $H_2O$ was added (300 mL) and the reaction was stirred/swirled vigorously. The reaction was filtered through an oversized Buchner funnel, and the brown precipitate was washed with $H_2O$ (300 mL) and ether (200 mL) and dried overnight on the funnel. To the crude dimethyl ether xanthone (3.27 g, 12.0 mmol) in dimethylformamide (60 mL) was added 3-chloro-3-methyl-1-butyne (11.8 g, 36.1 mmol),

KI (1.0 g, 6.01 mmol), and $Cs_2CO_3$ (11.8 g, 36.1 mmol). The reaction was heated at 50°C for 19 hours, cooled to room temperature, and then placed in an ice-bath. HCl (2 mol/L) was added until the reaction was quenched and no more foaming was observed. The mixture was then diluted with $CH_2Cl_2$ (200 mL) and the layers were separated. The organic layer was washed with saturated NaCl (50 mL), dried ($Na_2SO_4$), and concentrated under reduced pressure. The crude product was purified by column chromatography (60% ethyl acetate/hexane) to yield 3.50 g (75%) of a yellow solid. $^1$H NMR (250 MHz, $CDCl_3$) δ 7.88 (d, 1 H, $J$ = 5.12 Hz), 7.20–7.02 (m, 3 H), 4.00 (s, 3 H), 3.98 (s, 3 H), 2.78 (s, 1 H), 1.80 (s, 6 H); $^{13}$C NMR (62.5 MHz) δ 175.1, 161.4, 161.2, 158.7, 147.8, 145.2, 123.1, 117.6, 115.5, 114.5, 107.6, 98.7, 98.6, 84.6, 76.9, 72.6, 56.2, 29.4; mass spectrum (CI) $m/z$ + 1 339.1233 [$C_{20}H_{19}O_5$ (M + 1) requires 339.1232] 339 (base), 273.

**1,5-Dimethoxy-3-(3′ 3′ -Dimethylpropenoxy) Xanthone.** 5% Pd/$CaCO_3$ poisoned with lead (Lindlar's catalyst; 1.37 g, 0.642 mmol) was added to a solution of alkyne (2.17 g, 6.42 mmol) and quinoline (3.5 mL) in benzene (200 mL). The reaction flask was evacuated and then back-filled with $H_2$ from a balloon. The reaction was stirred under $H_2$ for 2 hours. (The reaction can be monitored by the $^1$H NMR of small aliquots that have been filtered through celite and concentrated, observing the disappearance of the alkyne proton or the appearance of the olefin protons.) After 2 hours, more Pd catalyst was added (0.5 g) and the reaction was stirred 1.5 hours more under $H_2$. The reaction was filtered through a pad of celite, washed with ethyl acetate (300 mL), and concentrated under reduced pressure. The residue was dissolved in $CH_2Cl_2$ (100 mL), washed with 2 mol/L HCl (4 × 200 mL) and saturated $NaHCO_3$, dried ($Na_2SO_4$), and concentrated under reduced pressure to yield 1.65 g (76%) of a yellow solid. $^1$H NMR (250 MHz, $CDCl_3$) δ 7.84 (d, 1 H, $J$ = 8.5 Hz), 7.25–7.11 (m, 2 H), 6.71 (s, 1 H), 6.38 (s, 1 H), 6.16 (dd, 1 H, $J$ = 17.7, 10.9 Hz), 5.33–5.23 (comp, 2 H), 3.99 (s, 3 H), 3.93 (s, 3 H), 1.54 (s, 6 H); $^{13}$C NMR (62.5 MHz) δ 176.4, 162.1, 161.0, 158.3, 148.0, 145.2, 143.3, 123.0, 117.5, 114.4, 114.3, 107.8, 98.7, 80.9, 56.2, 56.1, 27.2; mass spectrum (CI) $m/z$ + 1 341.1388 [$C_{20}H_{20}O_5$ (M + 1) requires 341.1388] 339 (base), 273.

**1,5-Dimethoxy-4-(1,1-Dimethylpropene) Xanthone (3).** A suspension of the olefin (0.23 g, 0.67 mmol) in diethylaniline (55 mL) was heated to 200°C for 3 hours and cooled to room temperature. The reaction was filtered and the precipitate was washed with methanol to provide 2.3 g (60%) of **3** as a beige solid. $^1$H NMR (250 MHz, DMSO-$d_6$) δ 10.8 (br s, 1 H), 7.60–7.55 (d, 1 H, $J$ = 7.8 Hz), 7.39–7.35 (m, 1 H), 7.30–7.24 (m, 1 H), 6.43 (s, 1 H), 5.29–5.24 (m, 1 H), 3.94 (s, 3 H), 3.80 (s, 3 H), 3.46–3.28 (comp, 2 H), 3.01–2.65 (m, 6 H); $^{13}$C NMR (62.5 MHz) δ 174.2, 161.5, 159.7, 156.2, 148.4, 144.8, 131.1, 123.7, 123.3, 122.8, 116.7, 115.5, 107.7, 105.6, 95.6, 56.5, 56.4, 25.9, 21.9, 17.9; mass spectrum (CI) $m/z$ + 1 341.1389 [$C_{20}H_{21}O_5$ (M + 1) requires 341.1389] 341 (base).

**(±)-1,5-Dimethoxy-2′ -Isopropenyl Dihydrofuranoxanthone (4).** DMSO (118 mL) was added to a mixture of **3** (1.21 g, 3.56 mmol), Pd[$(CH_3CN)_4(BF)_2$] (0.79 g, 1.78 mmol), and benzoquinone (recrystallized from ethanol, 3.84 g, 35.6 mmol). The solution was stirred for 36 hours, poured into a separatory funnel containing $CH_2Cl_2$ (400 mL), and washed with $H_2O$ (2 × 300 mL). The layers were separated and the $H_2O$ layer was washed with $CH_2Cl_2$ (200 mL). The organic layers were combined and washed with saturated NaCl (200 mL), dried ($Na_2SO_4$), and concentrated under reduced pressure. The crude product was purified by column chromatography (50% ethyl acetate/hexane), loading the product on the column in a minimum amount of $CH_2Cl_2$ to afford 0.15 g chromene (12%) and 0.97 g (81%) of **4** as a white solid. $^1$H NMR (250 MHz, $CDCl_3$) δ 7.82 (d, 1 H, $J$ = 7.9 Hz), 7.25–7.06 (comp, 2 H), 6.30 (s, 1 H), 5.34 (app t, $J$ = 8.5 Hz, 1 H), 5.08 (s, 1 H), 4.92 (s, 1 H), 3.93 (s, 3 H), 3.91 (s, 3 H), 3.50 (dd, 1 H, $J$ = 9.8, 15.4 Hz), 3.15 (dd, 1 H, $J$ = 7.9, 15.4 Hz), 1.80 (s, 3 H); $^{13}$C NMR (62.5 MHz) δ 175.0, 165.6, 162.9, 154.2, 147.8, 144.8, 143.0, 123.9, 123.0, 117.7, 114.5, 112.5, 106.7, 104.6, 89.7, 88.0, 56.4, 56.2, 31.2, 16.9; mass spectrum (CI) $m/z$ + 1 339.1232 [$C_{20}H_{19}O_5$ (M + 1) requires 339.1236] 339 (base).

**(±)-(2′ *R*,3′ *R*)-1,5-Dimethoxy-3′,4′ -Dihydroxy Dihydrofuranoxanthone.** A solution of **4** (0.25 g, 0.74 mmol) in $CHCl_3$ (2.5 mL) was added to *N*-methyl morpholine oxide (0.10 g, 0.89 mmol) and $OsO_4$ in 1:1 $H_2O$/acetone (2 mL). The reaction was stirred for 2 hours until no starting material remained by TLC (ethyl acetate). TLC showed two diastereomers, the lower $R_f$ being the desired diastereomer **A**. The reaction was filtered and the precipitate was washed with $H_2O$ (5 mL) and acetone (2 mL) and collected to yield a diastereomeric mixture of (±)-diol (0.24 g, 96%). $^1$H NMR analysis showed a 2:1 mixture of diastereomers (**B:A**). $^1$H NMR **A** (250 MHz, DMSO-$d_6$) δ 7.61 (d, 1 H), 7.40–7.25 (comp, 2 H), 6.54 (s, 1 H), 5.00–3.98 (m, 1 H), 4.96–4.94 (m, 1 H), 4.73 (m, 1 H), 3.95 (s, 3 H), 3.84 (s, 3 H), 3.33–3.20 (comp, 3 H), 1.12 (s, 3 H); mass spectrum (CI) $m/z$ + 1 373.1277 [$C_{20}H_{21}O_7$ (M + 1) requires 373.1287] 373 (base). Diastereomeric ratio can be determined by the $^1$H NMR of the aromatic singlet proton: **A** = 6.54 ppm, **B** = 6.57 ppm.

**(±)-(2′*R*,3′*R*)-4′-*t*-Butylsilyloxy-1,5-Dimethoxy-3′-Hydroxy Dihydrofuranoxanthone (5).** A solution of diol (0.23 g, 0.62 mmol), *t*-butyldimethylsilylchloride (0.14 g, 0.93 mmol), imidazole (0.13 g, 1.9 mmol), and 4-dimethylaminopyridine (38 mg, 0.31 mmol) in dimethylformamide was heated with a heat gun to ~85°C and stirred overnight. TLC (ethyl acetate) showed that diol still remained, so excess *t*-butyldimethylsilylchloride (0.14 g), imidazole (0.13 g), and 4-dimethylaminopyridine (40 mg) were added. The reaction was heated with a heat gun in the same manner and stirred for 2 hours (twice). The reaction was concentrated under reduced pressure. The crude product was purified by two successive columns (10% ethyl acetate/$CH_2Cl_2$) to afford 127 mg (42%) of **5B**, 54 mg (18%) of a mixed fraction of **5A** and **5B**, and 54 mg (18%) of pure **5A**. $^1$H NMR **5A** (250 MHz, $CDCl_3$) δ 7.84 (d, 1 H, $J$ = 7.8 Hz), 7.25–7.09 (comp, 2 H), 6.3 (s, 1 H), 4.99 (app t, 1 H, $J$ = 9.0 Hz), 3.95 (s, 3 H), 3.90 (s, 3 H), 3.54 (s, 2 H), 3.44–3.27

(comp, 2 H), 1.13 (s, 3 H), 0.90 (s, 3 H), 0.09 (s; 6 H); $^{13}$C NMR (62.5 MHz) δ 175.1, 165.6, 162.7, 154.1, 147.9, 144.9, 123.9, 123.1, 117.7, 114.6, 106.7, 105.1, 89.8, 88.4, 86.4, 73.5, 67.4, 56.3, 26.9, 25.7, 19.9, −5.6; IR ($CH_2Cl_2$) $cm^{-1}$; mass spectrum (CI) *m/z* + 1 487.2141 [$C_{26}H_{35}O_7$ Si (M + 1) requires 487.2152] 487 (base).

**(±)-(2′*R*,3′*R*) *O*$^5$-Methyl Psorospermin (6).** Tetrabutylammonium fluoride (0.06 mL, 0.062 mmol) and **5A** (0.02 g, 0.041 mmol) in tetrahydrofuran (1.5 mL) were stirred for 10 minutes and then concentrated under reduced pressure. The crude product was dissolved in pyridine (0.5 mL) and cooled to 0°C, and mesyl chloride (100 μL) was added dropwise. The reaction was stirred for 30 minutes and monitored by TLC (ethyl acetate). More MsCl was added (20 μL) and the reaction was stirred 15 minutes. $H_2O$ was added (2 mL) and the mixture was extracted with $CHCl_3$. The cloudy organic layer was washed with 6 mol/L HCl (5 mL), dried ($Na_2SO_4$), and concentrated under reduced pressure. To the crude mesylate was added acetone (2 mL), 18-crown-6 (82 mg, 0.031 mmol), and $K_2CO_3$ (43 mg, 0.31 mmol). The white suspension was stirred vigorously until TLC (ethyl acetate) showed that no mesylate remained (1–3 hours). The reaction was decanted into a separatory funnel containing ethyl acetate (20 mL). The flask and remaining $K_2CO_3$ were washed with ethyl acetate (10 mL), which was added to the separatory funnel. The organic layer was washed with saturated NaCl (10 mL), dried ($Na_2SO_4$), and concentrated under reduced pressure. The crude product was purified by column chromatography (ethyl acetate), loading the product onto the column in $CH_2Cl_2$ to afford 7 mg (50%) of (±)-psorospermin methyl ether. The $^1$H NMR and the high-resolution mass spectral (HRMS) data correspond to that expected as well as to that reported previously (12). $^1$H NMR (250 MHz, $CDCl_3$) δ 7.84 (d, *J* = 6.3 Hz), 7.26–7.11 (complex, 2 H), 6.34 (s, 1 H), 4.85 (dd, 1 H, *J* = 9.9, 7.3 Hz), 4.12 (s, 3 H), 4.09 (s, 3 H), 3.54 (dd, 1 H, *J* = 15.4, 9.9 Hz), 3.34 (dd, 1 H, *J* = 15.4, 9.9 Hz), 2.95 (d, 1 H, *J* = 4.6 Hz), 2.71 (d, 1 H, *J* = 4.6 Hz), 1.43 (s, 3 H); $^{13}$C NMR (62.5 MHz) δ 175.1, 165.4, 163.0, 154.2, 147.9, 144.9, 123.9, 123.2, 117.8, 114.6, 105.5, 103.9, 89.8, 86.9, 57.7, 56.5, 56.3, 50.9, 28.8, 16.5; mass spectrum (CI) *m/z* + 1 355.1188 [$C_{20}H_{19}O_6$ (M + 1) requires 355.1182] 355, 341 (base).

**(±)-1-Hydroxy-2′-Isopropenyl-5-Methoxy Dihydrofuranoxanthone.** $BCl_3$ (1.0 mol/L in $CH_2Cl_2$, 0.30 mL, 0.30 mmol) was added dropwise over 5-second intervals to methyl ether **4** (0.10 g, 0.30 mmol) in $CHCl_3$ at 0°C. The reaction was stirred for 15 minutes and then warmed to room temperature. TLC (40% ethyl acetate/hexane) showed that **4** still remained. More $BCl_3$ (0.10 mL) was added dropwise at room temperature. After 15 minutes, TLC showed that **4** still remained, so $BCl_3$ (0.15 mL, followed by 50 μL) was added dropwise at room temperature. The reaction was poured into a separatory funnel containing $H_2O$ (20 mL) and extracted with $CH_2Cl_2$ (2 × 10 mL). The organic layers were combined, washed with saturated NaCl, and dried ($Na_2SO_4$). The crude product was purified by column chromatography, eluting with 40% ethyl acetate/hexane to afford 84 mg (88%) of **8** as a yellow solid. $^1$H NMR (250 MHz, $CDCl_3$) δ 13.1 (s, 1 H), 7.76 (d, 1 H, *J* = 6.0 Hz), 7.26–7.16 (comp, 2 H), 6.30 (s, 1 H), 5.37 (app t, 1 H, *J* = 8.5 Hz), 5.11 (s, 1 H), 4.95 (s, 1 H), 3.98 (s, 3 H), 3.50 (dd, 1 H, *J* = 15.3, 9.96 Hz), 3.18 (dd, 1 H, *J* = 15.3, 7.6 Hz), 2.04 (s, 3 H).

**(±)-1-Alkylether-2′-Isopropenyl-5-Methoxy Dihydrofuranoxanthone (8).** $Cs_2CO_3$ (80.0 mg, 0.25 mmol) was added to the phenol (40 mg, 0.12 mmol) and alkyl iodide (15 μL, 0.19 mmol) in dimethylformamide (3 mL) at room temperature. After 3 hours at 50°C, more alkyl iodide (10 μL) was added, and the reaction was stirred an additional 1 hour. HCl (2 mol/L) was added slowly until the reaction mixture was acidic by pH paper. After warming to room temperature, the reaction was diluted with $CH_2Cl_2$ (10 mL) and $H_2O$ (10 mL). The organic layer was washed with brine (400 mL), dried ($Na_2SO_4$), and concentrated under reduced pressure to provide a yellow solid. Column chromatography, eluting with 40% ethyl acetate/hexane, afforded 34 mg (79%) of ethoxy ether as a white solid.

**Isopropyl Analogue (8b).** $^1$H NMR (250 MHz, $CDCl_3$) δ 7.86 (d, 1 H, *J* = 6.3 Hz), 7.28–7.10 (comp, 2 H), 6.37 (s, 1 H), 5.37 (app t, 1 H, *J* = 8.5 Hz), 5.12 (s, 1 H), 4.96 (s, 1 H), 4.62 (m, 1 H), 3.97 (s, 3 H), 3.56 (dd, 1 H, *J* = 15.3, 9.7 Hz), 3.22 (dd, 1 H, *J* = 7.8, 15.3 Hz), 1.81 (s, 3 H), 1.49 (m, 6 H); $^{13}$C NMR (62.5 MHz) δ 175.1, 165.5, 161.5, 154.4, 147.9, 144.9, 143.2, 124.1, 123.0,117.8, 114.6, 112.6, 107.7, 104.5, 92.5, 88.1, 72.1, 56.3, 31.4, 21.9, 17.0; mass spectrum (CI) *m/z* + 1 357.1549 [$C_{22}H_{23}O_5$ (M + 1) requires 367.1545] 367, 154 (base).

**Ethyl Analogue (8a).** $^1$H NMR (250 MHz, $CDCl_3$) δ 7.86 (d, 1 H, *J* = 6.3 Hz), 7.25–7.08 (comp, 2 H), 6.33 (s, 1 H), 5.36 (app t, 1 H, *J* = 8.7 Hz), 5.10 (s, 1 H), 4.95 (s, 1 H), 4.15 (q, 2 H, *J* = 7.0 Hz), 3.96 (s, 3 H), 3.56 (dd, 1 H, *J* = 15.3, 9.7 Hz), 3.20 (dd, 1 H, *J* = 7.8, 15.3 Hz), 1.79 (s, 3 H), 1.55 (t, 3 H, *J* = 7.0 Hz); mass spectrum (CI) *m/z* + 1 353.1392 [$C_{21}H_{21}O_5$ (M + 1) requires 353.1389] 353, 307, 154 (base).

**(±)-(2′*R*,3′*R*)-1-Ethoxy-Psorospermin Methyl Ether (9a).** Procedure is the same as that used to make compounds **5** and **6**. $^1$H NMR (250 MHz, $CDCl_3$) δ 7.86 (d, 1 H, *J* = 6.3 Hz), 7.25–7.13 (comp, 2 H), 6.35 (s, 1 H), 4.83 (d, 1 H, *J* = 9.9, 7.3 Hz), 4.15 (q, 2 H, *J* = 7.0 Hz), 3.99 (s, 3 H), 3.49 (dd, 1 H, *J* = 15.4, 9.9 Hz), 3.20 (dd, 1 H, *J* = 15.4, 8.0 Hz), 2.95 (d, 1 H, *J* = 4.6 Hz), 2.72 (d, 1 H, *J* = 4.6 Hz), 1.55 (t, 3 H, *J* = 7.0 Hz).

**(±)-(2′*R*,3′*R*)-1-Isopropoxy-Psorospermin Methyl Ether (9b).** Procedure is the same as that used to make compounds 5 and 6. $^1$H NMR (250 MHz, $CDCl_3$) δ 7.86 (d, 1 H, *J* = 6.3 Hz), 7.26-7.12 (comp, 2 H), 6.36 (s, 1 H), 4.62 (m, 1 H), 3.98 (s, 3 H), 3.52 (dd, 1 H, *J* = 15.1, 7.1 Hz), 3.20 (dd, 1 H, *J* = 9.9, 15.1 Hz), 2.95 (d, 1 H, *J* = 4.6 Hz), 2.72 (d, 1 H, *J* = 4.6 Hz), 1.57-1.53 (comp, 6 H), 1.44 (s, 3 H); mass spectrum (CI) *m/z* + 1 383.1500 [$C_{22}H_{23}O_6$ (M + 1) requires 383.1495] 383 (base), 341, 154.

**Chiral Resolution of Racemic Mixtures of (±)-(2′*R*,3′*R*) and (±)-(2′*R*,3′*S*) *O*$^5$-Methyl Psorospermin.** The racemic mixtures of compound **6** were separated by normal-phase chiral chromatography using the Waters (Milford, MA) 600 pump controller and automated fraction collector. The mobile phase was an isocratic mixture of hexane/

**Table 1. $IC_{50}$ of (±)-(2′*R*,3′*R*) $O^5$-methyl psorospermin in solid tumors, leukemias, and lymphomas**

| Cell line | Origin | $O^5$-methyl psorospermin ($IC_{50}$, μmol/L) |
|---|---|---|
| Solid tumors | | |
| A2780 | Ovarian | 0.063 |
| A2780/CP70 (cisplatin resistant) | Ovarian | 0.473 |
| MCF-7 | Breast, adenocarcinoma | 0.610 |
| MCF-10A | Breast normal mammary | 5.350 |
| DU-145 | Prostate, brain metastasis | 0.304 |
| LNCaP | Prostate, lymph node metastasis | 0.460 |
| PEAZ-1 | Prostate, primary | 0.160 |
| PC-3 | Prostate, adenocarcinoma, metastasis | 0.280 |
| PC-3N | Prostate, N-cadherin positive | 0.130 |
| MiaPaCa-3 | Pancreas | 0.180 |
| NCI-H82 | Small cell lung cancer | 0.067 |
| Leukemias | | |
| 8226/S | Multiple myeloma | 0.036 |
| HL60 | Acute promyelocytic leukemia | 0.012 |
| HL60/AR (Adriamycin resistant) | Acute promyelocytic leukemia | 0.011 |
| K562 | Chronic myelogenous leukemia | 0.036 |
| K562/R (daunorubicin resistant) | Chronic myelogenous leukemia | 0.024 |
| Lymphomas | | |
| U937 | Lymphoma (Non-Hodgkin's lymphoma) | 0.057 |
| Granta | Mantle cell lymphoma | 0.002 |
| G4 | Mantle cell lymphoma | 0.002 |

isopropanol/1,2-dichloroethane (30:10:10) at a constant flow of 6.0 mL/min. The stationary phase was a Chirex (S)-VAL and DNAn 250 × 10.0 mm column by Phenomenex (Torrance, CA). The temperature was kept constant at 30°C with a Waters 600 column heater. Liquid chromatography-mass spectra were obtained by reverse-phase liquid chromatography using a Waters 2767 autosampler, 2525 pump, Sunfire $C_{18}$ 5 μm, 4.6 × 50 column and ZQ mass detection. Proton NMR spectra ($^1$H NMR) were recorded at ambient temperatures on a Varian (Palo Alto, CA) Mercury 400 MHz spectrometer, and chemical shifts are expressed in parts/million relative to tetramethylsilane as an internal standard. HRMS were measured by electrospray ionization-time of flight.

**(2′*R*,3′*R*) Psorospermin-5-Methyl Ether. 5,10-Dimethoxy-2-(2-Methyloxiran-2-yl)-1,2-Dihydrofuro[2,3-*c*] Xanthen-6-one.** $^1$H NMR ($CDCl_3$) δ 7.87 (dd, *J* = 8.4 Hz, 1.6 Hz, 1H), 7.23 (d, *J* = 8.4 Hz, 1H), 7.16 (dd, *J* = 8.0 Hz, 1.6 Hz, 1H), 6.38 (s, 1H), 4.88 (dd, *J* = 9.6 Hz, 7.2 Hz, 1H), 3.995 (s, 3H), 3.98 (s, 3H), 3.56 (dd, *J* = 15.2 Hz, 9.6 Hz, 1H), 3.36 (dd, *J* = 15.2 Hz, 6.8 Hz, 1H), 2.98 (d, *J* = 4.4 Hz, 1H), 2.74 (d, *J* = 4.8 Hz, 1H), 1.44 (s, 3H); liquid chromatography-mass spectroscopy *m/z* 355 ($MH^+$; $t_R$ 3.66 minutes); HRMS calculated for $C_{20}H_{19}O_6$ (M + 1) 355.1176, found 355.1178.

**(2′*R*,3′*S*) Psorospermin-5-Methyl Ether. 5,10-Dimethoxy-2-(2-Methyloxiran-2-yl)-1,2-Dihydrofuro[2,3-*c*] Xanthen-6-one.** $^1$H NMR ($CDCl_3$) δ 7.87 (dd, *J* = 8.4 Hz, 1.6 Hz, 1H), 7.24 (d, *J* = 8.4 Hz, 1H), 7.16 (dd, *J* = 8.4 Hz, 1.6 Hz, 1H), 6.38 (s, 1H), 4.92 (dd, *J* = 10.0 Hz, 8.0 Hz, 1H), 3.995 (s, 3H), 3.98 (s, 3H), 3.48 (dd, *J* = 15.2 Hz, 9.6 Hz, 1H), 3.32 (dd, *J* = 15.2 Hz, 7.2 Hz, 1H), 2.88 (d, *J* = 4.8 Hz, 1H), 2.76 (d, *J* = 4.8 Hz, 1H), 1.47 (s, 3H); liquid chromatography-mass spectroscopy *m/z* 355 ($MH^+$; $t_R$ 3.68 minutes); HRMS calculated for $C_{20}H_{19}O_6$ (M + 1) 355.1176, found 355.1172.

**(2′*S*,3′*R*) Psorospermin-5-Methyl Ether. 5,10-Dimethoxy-2-(2-Methyloxiran-2-yl)-1,2-Dihydrofuro[2,3-*c*] Xanthen-6-one.** $^1$H NMR ($CDCl_3$) δ 7.87 (dd, *J* = 8.0 Hz, 1.6 Hz, 1H), 7.24 (d, *J* = 8.0 Hz, 1H), 7.16 (dd, *J* = 8.0 Hz, 1.6 Hz, 1H), 6.38 (s, 1H), 4.92 (dd, *J* = 10.0 Hz, 8.0 Hz, 1H), 3.99 (s, 3H), 3.98 (s, 3H), 3.48 (dd, *J* = 15.2 Hz, 9.6 Hz, 1H), 3.32 (dd, *J* = 15.2 Hz, 7.2 Hz, 1H), 2.88 (d, *J* = 4.8 Hz, 1H), 2.76 (d, *J* = 4.8 Hz, 1H), 1.47 (s, 3H); liquid chromatography-mass spectroscopy *m/z* 355 ($MH^+$; $t_R$ 3.66 minutes); HRMS calculated for $C_{20}H_{19}O_6$ (M + 1) 355.1176, found 355.1170.

**(2′*S*,3′*S*) Psorospermin-5-Methyl Ether. 5,10-Dimethoxy-2-(2-Methyloxiran-2-yl)-1,2-Dihydrofuro[2,3-*c*] Xanthen-6-one.** $^1$H NMR ($CDCl_3$) δ 7.87 (dd, *J* = 8.0 Hz, 1.6 Hz, 1H), 7.23 (d, *J* = 8.0 Hz, 1H), 7.16 (dd, *J* = 8.0 Hz, 1.6 Hz, 1H), 6.38 (s, 1H), 4.88 (dd, *J* = 9.6 Hz, 7.2 Hz, 1H), 3.995 (s, 3H), 3.98 (s, 3H), 3.56 (dd, *J* = 15.2 Hz, 9.6 Hz, 1H), 3.36 (dd, *J* = 15.2 Hz, 6.8 Hz, 1H), 2.98 (d, *J* = 4.4 Hz, 1H), 2.74 (d, *J* = 4.8 Hz, 1H), 1.44 (s, 3H); liquid chromatography-mass spectroscopy *m/z* 355 ($MH^+$; $t_R$ 3.66 minutes); HRMS calculated for $C_{20}H_{19}O_6$ (M + 1) 355.1176, found 355.1175.

### Cytotoxicity Assay

*In vitro* cytotoxicity assays were done using the CellTiter 96 Non-Radioactive Cell Proliferation Assay (Promega Corp., Madison, WI). Cells were plated in 0.1 mL medium on day 0 in 96-well microtiter plates (Falcon, Becton Dickinson, Franklin Lakes, NJ). On day 1, serial dilutions (10 μL) of the test agent were added in replicates of four to the plates. After incubation for 4 days at 37°C in a humidified incubator, 20 μL of a 20:1 mixture of 3-(4,5-dimethylthiazol-2-yl)-5-(3-carboxymethoxyphenyl)-2- (4-sulfophenyl)-2H-tetrazolium, inner salt (2 mg/mL) and an electron coupling reagent, phenazine methosulfate (0.92 mg/mL in Dulbecco's PBS), was added to each well and incubated for 2 hours at 37°C. Absorbance was measured using a Wallac Victor2 1420 MultiLabel Counter (Perkin-Elmer, Boston, MA) at 490 nm. Data were expressed as the percentage of survival of control calculated from the absorbance corrected for background absorbance. The surviving fraction of cells was determined by dividing the mean absorbance values of the test agents by the mean absorbance values of untreated control. $IC_{50}$ values were determined using logarithmic regression analysis.

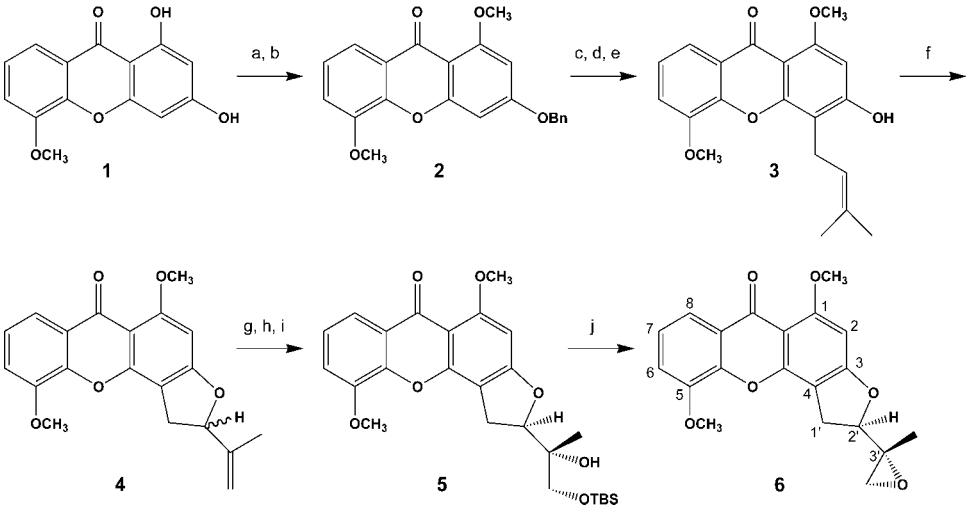


**Figure 2.** Synthesis of psorospermin methyl ether. *a,* BnBr, $Cs_2CO_3$, dimethylformamide 72%; *b,* methyl iodide, $Cs_2CO_3$, 66%; *c,* $FeCl_3$, $CH_2Cl_2$; 3-chloro-3-methyl-1-butyne, KI, $Cs_2CO_3$, dimethylformamide 75%; *d,* 5% $Pd/CaCO_3$, quinoline, $H_2$, $C_6H_6$ 76%; *e,* 200°C, diethylaniline 60%; *f,* $Pd[(CH_3CN)_4(BF)_2]$, benzoquinone, DMSO 81%; *g,* $OsO_4$, NMO, $H_2O$/acetone/$CHCl_3$ 96%; *h,t*-butyldimethylsilylchloride, imidazole, 4-dimethylaminopyridine, dimethylformamide 85°C; *i,* separation of diastereomers by column chromatography 27%; *j,* TBAF, tetrahydrofuran; MsCl, pyridine, $CHCl_3$; $K_2CO_3$, 18-crown-6, acetone 50%.

### DNA Alkylation Assay

The 5′-end-labeled oligo-A1 (d[CGCCGAAACAAGCGCTCATGAGCCCCGTATCAATGTATACGAGCCCGATCTTCCCCATCG]) was annealed with oligo-A2 (d[CGATGGGGAAGATCGGGCTCGTATACATTGATACGGGGCTCATGAGCGCTTGTTTCGGCG]), the complementary strand, by heating to 95°C and slowly cooled to room temperature. Labeled dsDNA was purified on an 8% native polyacrylamide gel. DNA was incubated with ~20 units human topoisomerase II in 20 μL reaction buffer [30 mmol/L Tris-HCl (pH 7.6), 3 mmol/L ATP, 15 mmol/L β-mercaptoethanol, 8 mmol/L $MgCl_2$, 60 mmol/L NaCl] at 30°C for 20 minutes in the presence of various concentrations of compounds. The reaction was terminated by adding 5 μg calf thymus DNA followed by phenol/chloroform extraction and ethanol precipitation. DNA samples were then subjected to piperidine treatment and 12% denaturing PAGE. The gels were dried and exposed on a phosphor screen. Imaging and quantification were done using a PhosphorImager and ImageQuant 5.1 software (both from Molecular Dynamics, Piscataway, NJ).

### Molecular Modeling, Docking, and Molecular Dynamics Simulations

Molecular graphics, structural manipulations, energy minimization, molecular docking, and molecular dynamics simulations were carried out as described previously (13). The obtained lowest global structure from molecular dynamics simulations was used for computing distances between N7 of $G^6$ and the -$CH_2$ carbon atom of each of the psorospermin isomers and for determining corresponding intermolecular binding energies (refs. 14, 15; summarized in Table 1).

### *In vivo* Studies

MiaPaCa tumor-bearing (average tumor volume, ~90 $mm^3$) female *nu/nu* mice were given testing compounds i.p. on schedules of (*a*) q3d × 4 for gemcitabine at 160 mg/kg, (*b*) qd × 5/2/5 for psorospermin at 1.25 mg/kg, and (*c*) qod × 10 for psorospermin at 2.5 mg/kg. Two groups were treated on the same schedules but with a combination of gemcitabine and psorospermin. Tumor measurements were taken with calipers twice weekly starting on day 1, and body weights were measured at the same time points. Tumor volumes were calculated from the standard formula: $W^2 \times L / 2$.

## Results

### Synthesis of Diastereomeric (±)-(2′*R*,3′*R*) $O^5$-Methyl Psorospermin

Approaches to the synthesis of (±)-(2′*R*,3′*R*) psorospermin (**1**) have been investigated by two different groups of chemists (11, 12). Our approach used a novel asymmetrical Wacker-type cyclization to form an oleofin-substituted benzofuran (16). This intermediate was

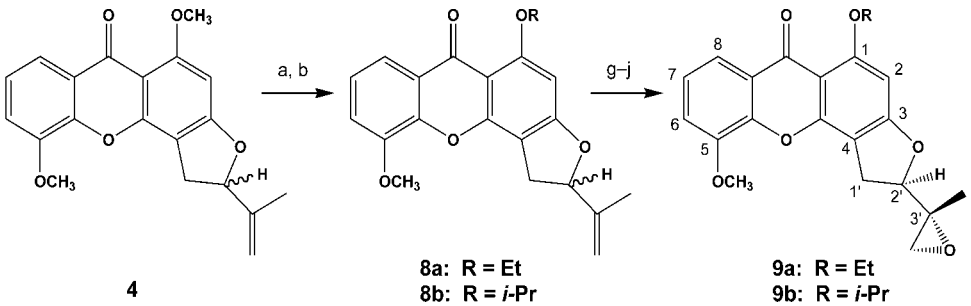


**Figure 3.** Synthesis of $O^1$-ethyl and $O^1$-isopropyl (±)-(2′*R*,3′*R*) psorospermin analogues. *a,* $BCl_3$, $CH_2Cl_2$ 88%; *b,* Et or *i*-Pr, $Cs_2CO_3$, dimethylformamide 79%.

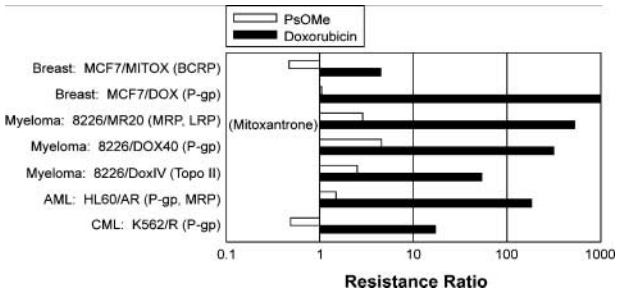


**Figure 4.** Resistance ratio of sensitivity of matched cell lines to doxorubicin and $O^5$-methyl psorospermin (*PsOMe*). *Open columns*, $O^5$-methyl psorospermin; *filled columns*, doxorubicin (*DOX*) and mitoxantrone (*MITOX*).

manipulated into many desired analogues before installing the labile epoxide. The synthesis of psorospermin methyl ether was accomplished as shown in Fig. 2. Condensation of dimethoxybenzoic acid and phloroglucinal provided the xanthone core **1** (11). Selective protection of the phenol, which is not chelated to the ketone with benzyl bromide, was followed by alkylation with methyl iodide to provide **2**. Debenzylation with $FeCl_3$ followed by reaction with 3-chloro-3-methyl-1-butyne afforded the alkyne. Hydrogenation to the olefin with Lindlar's catalyst and Claisen rearrangement afforded **3**. Allylphenol **3** was subject to asymmetrical oxidative Wacker cyclization based on reports by Hayashi et al. using ip-boxax chiral ligands (17, 18). To our surprise, under the reported conditions, only formation of the six-membered ring chromene was observed. However, changing the solvent from methanol to DMSO afforded benzodihydrofuran **4** as the major product. Disappointingly, no enantioselectivity was observed under the reaction conditions. Therefore, the reaction was run without chiral ligand to afford an 81% yield of racemic **4**. Dihydroxylation provided the diol. Due to its insolubility, the diol was silyated, so that the diastereomers could be separated by column chromatography to provide pure **5**. Deprotection with tetrabutylammonium fluoride, followed by reaction with mesyl chloride and formation of the epoxide, provided (±)-(2′*R*,3′*R*) $O^5$-methyl psorospermin (**6**). The undesired diastereomer of **5** was also subject to epoxide formation to provide the other diastereomer [(±)-(2′*R*,3′*S*)] of $O^5$-methyl psorospermin.[7]

$O^1$-ethyl and $O^1$-isopropyl (±)-(2′*R*,3′*R*) psorospermin analogues were synthesized as shown in Fig. 3. Compound **4** was subject to demethylation with $BCl_3$ followed by transformation to the ethyl or isopropyl derivative. The olefins **8a** and **8b** were subjected to the same conditions as shown in Fig. 2 to provide the desired ethyl and isopropyl analogues **9a** and **9b**.

[7] L. Hurley and I. Fellows, unpublished results.

### *In vitro* Evaluation of the (±)-(2′*R*,3′*R*) $O^5$-Methyl Psorospermin in Solid Tumors, Lymphomas, and Drug-Sensitive versus Drug-Resistant Leukemias

The (±)-(2′*R*,3′*R*) $O^5$-methyl psorospermin diastereomer containing the natural isomer was evaluated in a range of solid tumors, lymphomas, and drug-sensitive and drug-resistant leukemias (Table 1). In solid tumors, $O^5$-methyl psorospermin is particularly active in ovarian and small cell lung cancer (~60–70 nmol/L). MCF-10A (normal breast cancer cell line) is 10 times less sensitive than MCF-7. It is also extremely potent (2 nmol/L) in mantle cell lymphomas.

The activity of psorospermin against drug-resistant leukemias was reported previously (2). To further substantiate this, a comparison of the activity of (±)-(2′*R*,3′*R*) $O^5$-methyl psorospermin in a wider range of both drug-sensitive and drug-resistant solid tumor, myeloma, and leukemia cell lines was made. (Doxorubicin or mitoxantrone were used as reference compounds.) The results in Fig. 4 show that, in comparison with doxorubicin and mitoxantrone, (±)-(2′*R*,3′*R*) $O^5$-methyl psorospermin shows resistance ratios in drug-sensitive versus drug-resistant cell lines of <5 in comparison with resistance ratios in the same matched cell lines of between ~10 and 1,000 for doxorubicin and mitoxantrone.

The *in vitro* potency of the (±)-(2′*R*,3′*S*) and (±)-(2′*R*,3′*R*) $O^5$-methyl psorospermin diastereomeric pairs was compared in five different cell lines.[7] Overall,

**Table 2. Comparison of cytotoxicity of $O^5$-methyl psorospermin with 9a and 9b**

| Cell line | Origin | $IC_{50}$ (μmol/L) | | |
|---|---|---|---|---|
| | | (±)-(2′*R*,3′*R*) $O^5$-methyl psorospermin | **9a** | **9b** |
| 8226/S | Multiple myeloma | 0.036 | 0.095 | 0.200 |
| HL60 | Acute promyelocytic leukemia | 0.012 | 0.037 | 0.076 |
| HL60/AR (Adriamycin resistant) | Acute promyelocytic leukemia | 0.011 | 0.045 | 0.110 |
| K562 | Chronic myelogenous leukemia | 0.036 | 0.081 | 0.076 |
| K562/R (daunorubicin resistant) | Chronic myelogenous leukemia | 0.024 | 0.062 | 0.145 |
| A2780 | Ovarian | 0.063 | 0.133 | 0.245 |
| A2780/CP70 | Ovarian | 0.473 | 0.613 | 1.453 |
| DU 145 | Prostate, brain metastasis | 0.304 | 0.685 | 0.751 |
| LNCaP | Prostate, lymph node metastasis | 0.460 | 0.630 | 1.400 |
| MiaPaCa-2 | Pancreas | 0.180 | 0.570 | 0.610 |

**Table 3. 3-(4,5-Dimethylthiazol-2-yl)-5-(3-carboxymethoxyphenyl)-2- (4-sulfophenyl)-2H-tetrazolium, inner salt cytotoxicity data**

| Cell line | Tumor type | $O^5$-methyl psorospermin ($IC_{50}$, μmol/L) | | | |
|---|---|---|---|---|---|
| | | 2′*R*,3′*R* | 2′*R*,3′*S* | 2′*S*,3′*R* | 2′*S*,3′*S* |
| Solid tumors | | | | | |
| HeLa | Cervical, adenocarcinoma | 0.390 (1)* | 2.500 (2) | 3.200 (3) | 4.450 (4) |
| MCF-7 | Breast, adenocarcinoma | 0.430 (1) | 0.570 (3) | 0.550 (2) | 2.720 (4) |
| MCF-7/DOX (doxorubicin resistant) | Breast, adenocarcinoma | 0.190 (1) | 0.690 (3) | 0.550 (2) | 2.220 (4) |
| DU 145 | Prostate, brain metastasis | 0.230 (1) | 0.670 (3) | 0.570 (2) | 2.510 (4) |
| MiaPaCa-2 | Pancreas | 0.100 (1) | 0.360 (2) | 0.380 (3) | 1.180 (4) |
| H522 | Non–small cell lung | 0.280 (1) | 1.350 (3) | 0.770 (2) | 2.770 (4) |
| Leukemias | | | | | |
| HL60 | Acute promyelocytic leukemia | 0.016 (3) | 0.014 (2) | 0.009 (1) | 0.021 (4) |
| HL60/AR (Adriamycin resistant) | Acute promyelocytic leukemia | 0.013 (2) | 0.012 (1) | 0.016 (3) | 0.022 (4) |
| K562 | Chronic myelogenous leukemia | 0.054 (1) | 0.286 (3) | 0.169 (2) | 0.595 (4) |
| K562/R (daunorubicin resistant) | Chronic myelogenous leukemia | 0.036 (1) | 0.207 (3) | 0.100 (2) | 0.329 (4) |
| 8226 | Multiple myeloma | 0.072 (1) | 0.345 (3) | 0.221 (2) | 0.494 (4) |
| 8226/DOX1V (topoisomerase II mediated) | Multiple myeloma | 0.097 (1) | 0.366 (3) | 0.280 (2) | 1.100 (4) |
| 8226/DOX40 | Multiple myeloma | 0.037 (1) | 0.229 (3) | 0.174 (2) | 0.335 (4) |
| Lymphomas | | | | | |
| Granta | Mantle cell lymphoma | 0.005 (1) | 0.050 (3) | 0.031 (2) | 0.071 (4) |
| NCEB-1 | Non-Hodgkin's lymphoma | 0.051 (3) | 0.038 (1) | 0.047 (2) | 0.110 (4) |
| U937 | Histiocytic lymphoma | 0.035 (1) | 0.260 (3) | 0.190 (2) | 0.570 (4) |

*Number in parentheses indicates ranking among the four enantiomers.

the diastereomer (±)-(2′*R*,3′*R*) containing the isomer having the same stereochemistry as the natural product is about two times more potent than the (±)-(2′*R*,3′*S*) diastereomer.

To assess the effect of steric bulk at the $O^1$-phenolic position on the biological activity of $O^5$-methyl psorospermin, ethyl and isopropyl analogues were prepared (see Fig. 3). In comparison with the (±)-(2′*R*,3′*R*) $O^5$-methyl psorospermin, the corresponding diastereomers of the $O^1$-ethyl (**9a**) and $O^1$-isopropyl (**9b**) were about two and four times less potent in cytotoxic activity, showing that the small methyl substituent has optimal activity (Table 2). The $O^1$-phenolic compound was unstable and therefore could not be evaluated.

### Chiral Resolution of the Racemic Mixtures of (±)-(2′*R*,3′*R*) and (±)-(2′*R*,3′*S*) $O^5$-Methyl Psorospermin

Normal-phase chiral chromatography using Chirex (S)-VAL and DNA in a column was used to provide the four chiral $O^5$-methyl psorospermin isomers. The optical purity of the four $O^5$-methyl psorospermin was 97% (*RR*), 94% (*RS*), 92% (*SR*), and 94% (*SS*).

### Comparison of the *In vitro* Activity of the Four Chiral $O^5$-Methyl Psorospermin Isomers

The four chiral $O^5$-methyl psorospermin isomers were evaluated for *in vitro* activity against a range of solid and hematopoietic tumors, including lymphomas and drug-sensitive and drug-resistant leukemia cell lines (Table 3). In many cases, the same cell lines were used previously in the evaluation of (±)-(2′*R*,3′*R*) $O^5$-methyl psorospermin (see Table 1). The results with the four chiral $O^5$-methyl psorospermin isomers show that, with three exceptions, the isomer (2′*R*,3′*R*) having the same stereochemistry as the natural product was the most active of the four enantiomers and the (2′*S*,3′*S*) was always least active. In the majority of cases, the (2′*S*,3′*R*) isomer was more active than the (2′*R*,3′*S*) isomer. Figure 5 shows a comparison of the potency of all four isomers in the various cell lines, in order of relative potency.

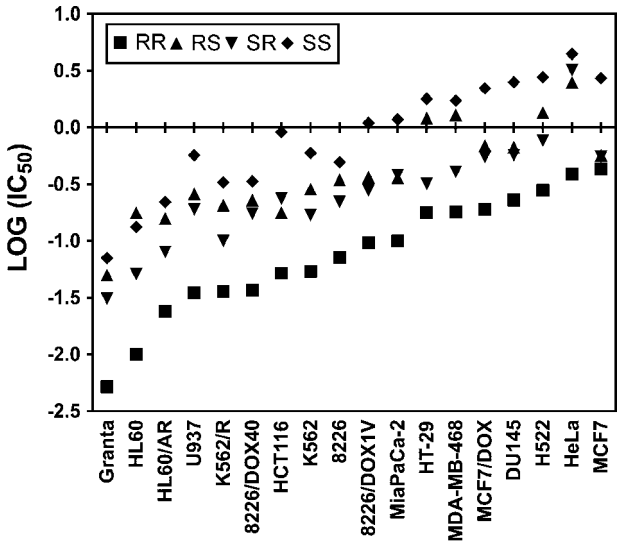


**Figure 5.** Comparison of the *in vitro* potency of the four chiral isomers of $O^5$-methyl psorospermin in order of increasing cytotoxic potency. *Blue diamonds,* (2′*R*,3′*R*); *red squares,* (2′*R*,3′*S*); *green triangles,* (2′*S*,3′*R*); *orange circles,* (2′*S*,3′*S*).

### Comparison of the Potency of the Topoisomerase II–Mediated Site-Directed DNA Alkylation of the Four Chiral $O^5$-Methyl Psorospermin Isomers

The topoisomerase II–mediated site-directed DNA alkylation by (2′*R*,3′*R*) $O^5$-methyl psorospermin and its three chiral isomers (2′*S*,3′*S*), (2′*R*,3′*S*), and (2′*S*,3′*R*) was determined by a strand breakage assay (4). A 60-bp duplex DNA, which contained a single topoisomerase II cleavage site, was incubated with increasing concentrations of all compounds in the presence and absence of human topoisomerase II (10). Piperidine heat treatment of the samples was then used to generate strand breakage products, which results from the depurination of the N7-alkylated guanine (Fig. 6A). In the absence of topoisomerase II, there was no significant DNA alkylation by any of the compounds (Fig. 6A, *left*); however, in the presence of human topoisomerase II, considerably more DNA alkylation took place at one specific guanine site, which is located at the topoisomerase II–mediated cleavage site (Fig. 6A, *right*; ref. 4). Quantification of the results from Fig. 6A is shown in Fig. 6B. This histogram shows that the enantiomer with the naturally occurring (2′*R*,3′*R*) stereochemistry had the most potent topoisomerase II–induced DNA strand break, with the (2′*S*,3′*S*) isomer being the least active. The (2′*R*,3′*S*) and (2′*S*,3′*R*) isomers had intermediate activity, with the (2′*S*,3′*R*) isomer being almost twice as potent as the (2′*R*,3′*S*) isomer. Although this hierarchy of activity mirrors that of the biological potency, the relative degrees of potency are quite different. There is a 30-fold difference in DNA strand breakage activity between (2′*R*,3′*R*) and (2′*S*,3′*S*) but only ~10-fold difference in biological potency (Table 3).

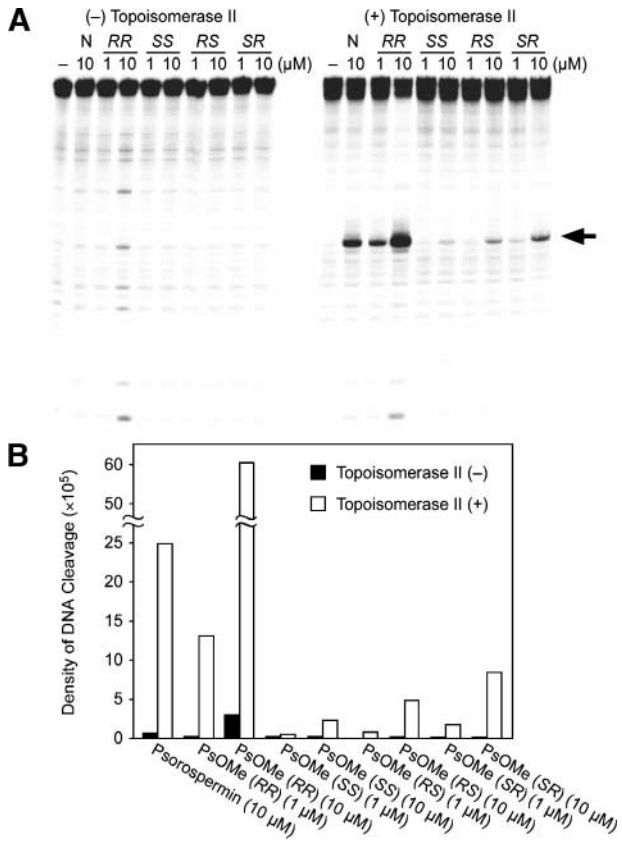


**Figure 6.** DNA alkylation in the presence and absence of topoisomerase II. **A,** autoradiogram of denaturing polyacrylamide gel showing the site-directed DNA alkylation by psorospermin and $O^5$-methyl psorospermin isomers in the presence and absence of topoisomerase II (*N,* natural product; *RR,* 2′*R*,3′*R*; *SS,* 2′*S*,3′*S*; *RS,* 2′*R*,3′*S*; *SR,* 2′*S*,3′*R*). **B,** graphical representation of the quantification of the extent of DNA alkylation in the presence and absence of topoisomerase II. Strand breakage products (**A,** *arrow*) were quantified.

**Table 4. Binding energies and distances between N7 of $G^6$ and -$CH_2$ of psorospermin in four enantiomers**

| Psorospermin | Binding energy (kcal/mol) | Distance between N7 of $G^6$ and -$CH_2$ of psorospermin (Å) |
|---|---|---|
| (2′*R*,3′*R*) | −53.96 | 3.95 |
| (2′*R*,3′*S*) | −49.81 | 4.82 |
| (2′*S*,3′*R*) | −51.43 | 4.09 |
| (2′*S*,3′*S*) | −47.29 | 4.94 |

### Molecular Modeling of the Four Chiral Isomers of Psorospermin

The high-resolution X-ray crystal structure of the d[CGTAC$^5$G$^6$/C$^7$G$^8$TACG] duplex DNA complexed with two molecules of doxorubicin was used as a template for this study (13). As described previously (13), psorospermin was substituted for one of the doxorubicin molecules, and after the psorospermin position was refined using an AMBER force field, the entire molecule was subjected to energy minimization. (Although psorospermin rather than $O^5$-methyl psorospermin was used in this molecular modeling study, we do not anticipate that the relative distance and/or binding energies will be significantly affected by this structural modification.) The binding energies for the four enantiomers are shown in Table 4 together with the corresponding distances between N7 of $G^6$ and the -$CH_2$ carbon of the epoxide ring obtained from final minimized models (see supporting information).[8] The results show that the lowest binding energy and shortest distance correspond to the (2′*R*,3′*R*) isomer, with the (2′*S*,3′*S*) isomer having the highest binding energy and longest intermolecular distance. This correlates with the hierarchy of the results from the DNA strand breakage assay and the *in vitro* biological potency for the four enantiomerically pure compounds. The (2′*R*,3′*S*) and (2′*S*,3′*R*) isomers, which have intermediate binding energies and intermolecular distances, also mirror the order of relative potencies from the two experimental results (Table 3; Fig. 5).

[8] Supplementary material for this article is available at Molecular Cancer Therapeutics Online (http://mct.aacrjournals.org).

### *In vivo* Activity of Psorospermin against MiaPaCa, a Pancreatic Cancer Model: A Combination Study with Psorospermin and Gemcitabine

In an *in vivo* study, combinations of psorospermin and gemcitabine were compared with each single agent given alone. The dosing schedule for drugs (psorospermin and gemcitabine) given i.p. was as shown in Fig. 7A. Tumor volume (Fig. 7A) and mean body weight (Fig. 7B) were determined for each group (i.e., psorospermin alone at 1.25 and 2.5 mg/kg, gemcitabine at 160 mg/kg, and the combinations at each dose level). The combination of psorospermin at 2.5 mg/kg with gemcitabine gave a significantly greater inhibition of tumor growth than either gemcitabine or psorospermin given alone (Fig. 7B). No weight loss above 10% occurred in any of the five groups of treated animals.

## Discussion

In this contribution, we have achieved the synthesis of the (±)-(2′*R*,3′*R*) $O^5$-methyl psorospermin in sufficient yield to evaluate their cytotoxicity in a range of solid and hematopoietic tumor cell lines, and through the availability of the four chiral $O^5$-methyl psorospermin isomers, we have correlated the biological potency and topoisomerase II–induced alkylation of DNA with the results of molecular modeling of the psorospermin isomers bound by intercalation in duplex DNA (see Fig. 8). There is reasonable correlation in each case.

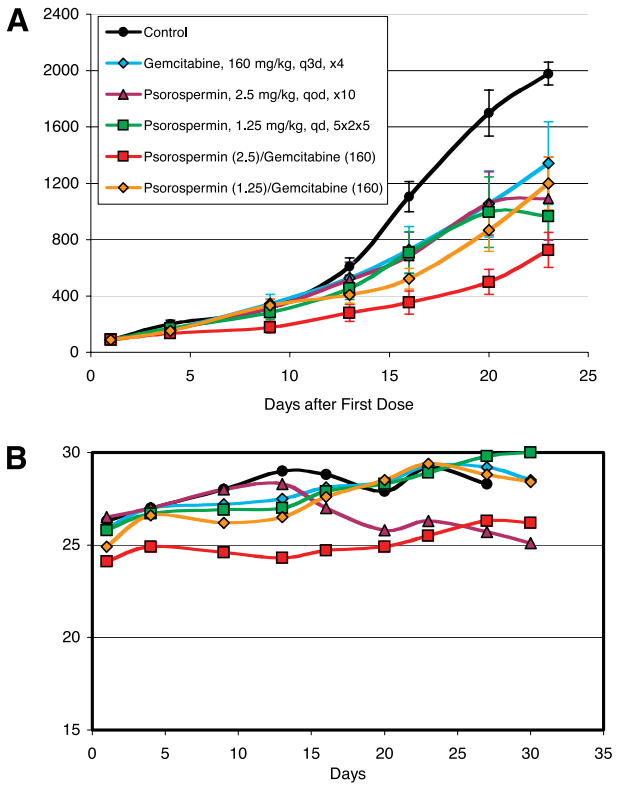


**Figure 7.** *In vivo* activity (**A**) and mean body weight (**B**) of psorospermin-treated mice with a MiaPaCa pancreatic tumor model. The dosing schedule for each group of 10 mice was as shown in **A**.

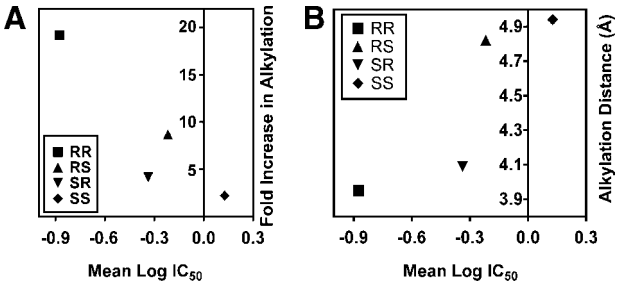


**Figure 8.** Linear plots of (**A**) fold increase in alkylation and (**B**) alkylation distance (Å) against mean 3-(4,5-dimethylthiazol-2-yl)-5-(3-carboxymethoxyphenyl)-2- (4-sulfophenyl)-2H-tetrazolium, inner salt. Results are from Tables 3 and 4 and Fig. 6.

The initial observations made by Kupchan et al. (1), that psorospermin is active in drug-resistant cell lines, has been confirmed and broadened to show equal or better activity in cell lines in which resistance is mediated by P-glycoprotein, multidrug resistance protein, lung resistance protein, topoisomerase II, breast cancer resistance protein, or combinations of these (e.g., P-glycoprotein/multidrug resistance protein) in comparison with doxorubicin or mitoxantrone. This is a significant finding because drug resistance is a great problem in cancer chemotherapy.

There is further evidence that topoisomerase II, or another DNA-binding protein that structurally modifies DNA, may be instrumental in facilitating a critical alkylation on DNA, because the hierarchy of topoisomerase II–induced alkylation mirrors that of the relative potency of *in vitro* activity of the four enantiomers of psorospermin.

Psorospermin has been evaluated in several tumor xenograft models, including the MiaPaCa pancreatic cancer model, a very hard to treat model generally considered an excellent predictor of the clinical efficacy of new agents. Psorospermin given was as effective as gemcitabine, the only clinically approved treatment for pancreatic cancer, at slowing tumor growth. In addition, this highest dose of psorospermin in combination with the highest effective dose of gemcitabine produced a slowing of tumor growth that was at least additive.

Based on *in vivo* activity against the MiaPaCa pancreatic cell line, a psorospermin analogue is in preclinical evaluation. These studies will be published in due course.

### Acknowledgments

We thank David Bishop for preparing, proofreading, and editing the final version of the article and figures.

### References

1. Kupchan SM, Streelman DR, Sneden AT. Psorospermin, a new antileukemic xanthone from *Psorospermum febrifugum*. J Nat Prod 1980;43:296–301.

2. Cassady JM, Baird WM, Chang CJ. Natural products as a source of

potential cancer chemotherapeutic and chemopreventive agents. J Nat Prod 1990;53:23–41.

**3.** Schwaebe MK, Moran TJ, Whitten JP. Total synthesis of psorospermin. Tetrahedron Lett 2005;46:827–9.

**4.** Hansen M, Lee SJ, Cassady JM, Hurley LH. Molecular details of the structure of a psorospermin-DNA covalent/intercalation complex and associated DNA sequence selectivity. J Am Chem Soc 1996;118:5553–61.

**5.** Kwok Y, Zeng Q, Hurley LH. Topoisomerase II-mediated site-directed alkylation of DNA by psorospermin and its use in mapping other topoisomerase II poison binding sites. Proc Natl Acad Sci U S A 1998;95:13531–6.

**6.** Permana PA, Ho DK, Cassady JM, Snapka RM. Mechanism of action of the antileukemic xanthone psorospermin: DNA strand breaks, abasic sites, and protein-DNA cross-links. Cancer Res 1994;54:3191–5.

**7.** Wang J. DNA topoisomerases. Annu Rev Biochem 1996;65:635–92.

**8.** Watt PM, Hickson ID. Structure and function of type II DNA topoisomerases. Biochem J 1994;303:681–95.

**9.** Osheroff N, Zechiedrich EL, Gale KC. Catalytic function of DNA topoisomerase II. BioEssays 1991;13:269–75.

**10.** Kwok Y, Hurley LH. Topoisomerase II site-directed alkylation of DNA by psorospermin and its effect on topoisomerase II-mediated DNA cleavage. J Biol Chem 1998;273:33020–6.

**11.** Cassady JM, Byrn SR, McKenzie AT, Ho DK. $O^5$-methyl-(±)-(2′*R*,3′*S*)-psorospermin. J Org Chem 1987;52:342–7.

**12.** Streelman DR. The chemistry of some potent antileukemic principles from plants. Ph.D. thesis. Charlottesville (VA): University of Virginia; 1977.

**13.** Kim MY, Na Y, Vankayalapati H, Gleason-Guzman M, Hurley LH. Design, synthesis, and evaluation of psorospermin/quinobenzoxazine hybrids as structurally novel antitumor agents. J Med Chem 2003;46:2958–72.

**14.** Åqvist J, Medina C, Samuuelson JE. New method for predicting binding affinities in computer-aided drug design. Protein Eng 1994;7:385–91.

**15.** Åqvist J. Calculation of absolute binding free energies for charged ligands and effects of long-range electrostatic interactions. J Comput Chem 1996;17:1587–97.

**16.** Hayashi T, Uozumi Y, Kato K. Kyota H, Ogasawara M. Design and preparation of 3,3′-disubstituted 2,2′-bis(oxazolyl)o1,1′binaphthyls (boxax): new chiral bis(oxazoline) ligands for catalytic asymmetric Wacker-type cyclization. J Org Chem 1999;64:1620–5.

**17.** Hayashi T, Uozumi Y, Kato K. Cationic palladium/boxax complexes for catalytic asymmetric Wacker-type cyclization. J Am Chem Soc 1998;63:5071–5.

**18.** Hayashi T, Uozumi Y, Kato K. Catalytic asymmetric Wacker-type cyclization. J Am Chem Soc 1997;119:5063–4.

Molecular Cancer Therapeutics

# Determination of the importance of the stereochemistry of psorospermin in topoisomerase II–induced alkylation of DNA and *in vitro* and *in vivo* biological activity

Ingrid M. Fellows, Michael Schwaebe, Thomas S. Dexheimer, et al.

*Mol Cancer Ther* 2005;4:1729-1739.